

Letters

Characterization of Superhydrophobic Materials Using Multiresonance Acoustic Shear Wave Sensors

Sun Jong Kwoun, Ryszard M. Lec, Richard A. Cairncross, Pratik Shah, and C. Jeffrey Brinker

Abstract—Various superhydrophobic (SH) surfaces, with enhanced superhydrophobicity achieved by the use of nanoparticles, were characterized by a new acoustic sensing technique using multiresonance thickness-shear mode (MTSM) sensors. The MTSM sensors were capable of differentiating SH properties created by nano-scale surface features for film, exhibiting similar macroscopic contact angles.

I. INTRODUCTION

IN recent years, a variety of synthetic approaches have been developed to create so-called superhydrophobic (SH) surfaces characterized normally by high static contact angles of water ($> 150^\circ$) [1]–[4]. Superhydrophobicity depends on surface roughness and surface chemistry, but to date rigorous structure-property relationships have not been established, especially the relationship between static and dynamic properties and how superhydrophobicity is influenced by nanoscale structural features. In this paper we use high-frequency shear acoustic waves generated by a piezoelectric quartz resonator thickness-shear mode (TSM) sensor to interrogate SH surfaces loaded with liquid media. For the TSM operating in the frequency range of 1 to ~ 100 MHz, the depth of penetration is on the order of tens to thousands of nanometers [5]; therefore, these sensors are sensitive to nanoscale interfacial phenomena and processes. Moreover, because the depth of penetration decreases with increasing TSM frequency, a multiresonance excitation of the sensor allows spatial interrogation of the interface with controllable interrogation depth. The purpose of this investigation is to evaluate the multiresonance TSM sensing technique to study the dynamic behavior of the SH/H₂O interface and to correlate the multiresonance TSM (MTSM) response with microscopic and nanoscopic features of SH surfaces. Although all the SH surfaces in this study had similar macroscopic wettability (optical contact angle $\sim 150^\circ$), MTSM showed different responses, depending on the surface treatments and film morphology. Thus, MTSM sensing may provide a new means of probing the functional behavior of SH films and help establish needed structure-property relationships.

Manuscript received January 10, 2006; accepted February 16, 2006.

S. J. Kwoun, R. M. Lec, and R. A. Cairncross are with Drexel University, Philadelphia, PA 19104 (e-mail: sunkwoun@gmail.com).

P. Shah and C. J. Brinker are with the University of New Mexico, Albuquerque, NM 87131.

II. EXPERIMENT

The TSM sensors were 10 MHz fundamental resonant frequency quartz crystals AT-cut and coated initially with gold electrodes on both sides. Five samples of varying hydrophobicity were prepared by coating the sensors and subjecting the coating to various surface treatments (Table I summarizes the sample preparation). Sample 1 was a bare TSM sensor and Samples 2 to 4A were coated with SH coatings of increasing hydrophobicity. Sample 2 was coated with TFPTMOS (trifluoropropyltrimethoxysilane) to produce a low-surface, free energy with submicron-scale roughness [4]. Sample 3 also had a TFPTMOS coating but was further treated with HMDS (hexamethyldisilazane) to derivatize any remaining hydroxyl groups with hydrophobic trimethyl silyl Si(CH₃)₃ groups on the surface. Sample 4A was prepared by the same techniques as Sample 3 but with the addition of silica nanoparticles (2% by weight) to the TFPTMOS coating, followed by treatment with HMDS. Sample 4B is the same MTSM sensor and coating as Sample 4A but after exposure to ultraviolet (UV)/ozone to reduce its hydrophobicity. All the SH samples were prepared in the laboratory at the University of New Mexico.


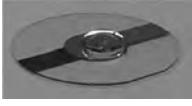

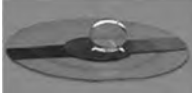
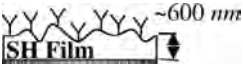
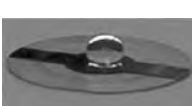

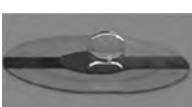


The samples were characterized for macroscopic contact angle and surface roughness. Contact angle was measured by the sessile drop method [6]. The surface topology and roughness of samples was measured using atomic force microscopy (AFM) [7]. The AFM images of the SH surfaces were obtained in $3 \mu\text{m} \times 3 \mu\text{m}$ areas and are shown in Fig. 1. The AFM software enables analysis of relative changes of surface area (Table I).

III. RESULTS AND DISCUSSION

The measured macroscopic optical contact angles of water on each of the samples are reported in Table I along with images of a water droplet resting on the sample surface. The contact angle increases from approximately 80° on the bare MTSM sensor to 140° to 155° for the SH coatings; Ultraviolet/ozone treatment reduces the contact angle to approximately 90° by changing the surface energy without affecting morphology. Samples 2, 3, and 4A are all SH with contact angles of 140° or more. The addition of silica nanoparticles in Sample 4A does not significantly increase the contact angle compared to Sample 3.

The surface area of the samples, as measured by AFM (Fig. 1), increases steadily from Sample 1 to 4A. The surface area of Sample 4A was approximately 46% larger than the initial surface area because of roughness resulting from the surface treatment. Samples 3 and 4A had similar surface areas and exhibited high contact angles characteristic of SH surfaces. So according to standard static characterization protocols, both Samples 3 and 4 were equally SH.

TABLE I
PHYSICAL PROPERTIES OF SH-FILMS DEPOSITED ON MTSM SENSORS.

Films and surface treatment	⁵	A ⁶	Schematic	Water drop on TSM sensors*
1. Gold, no surface treatment	80°	0%		
2. SH ¹ film, no surface treatment	140°	17%		
3. SH ¹ film + HMDS ² surface treatment	155°	43%		
4A. NP ³ mixed SH ¹ film + HMDS ² surface treatment	155°	46%		
4B. NP ³ mixed SH ¹ film + HMDS ² + UV ⁴ treatment	90°			

*These pictures show a water droplet on the various SH surfaces studied; however, for the MTSM experiments the sensors were completely covered by a ~4-mm layer of DI water. SH¹film: TFPTMOS. HMDS², (Y) hexamethyldisilazane, enhances hydrophobicity by replacing hydroxyl groups with trimethyl silyl groups. NP³, (●) silica nano particles (sizes between 22~66 nm) increase the surface roughness and geometrical SH mechanism. UV⁴, Ultraviolet light treatment reduces the water contact angle by removal of trimethyl silyl and trifluoropropyl groups. ⁵, contact angle measured optically. ⁶, increase in surface area relative to bare surface measured by AFM (%).

A network analyzer measurement system was used to monitor the frequency response of the MTSM sensor exposed to air or submersed in 200 μ l (about 4-mm depth) of deionized (DI) water [5]. All measurements were performed in an air-flow controlled chemical hood at room temperature (approximately 25°C \pm 0.1°C). The multi-harmonic frequency response characteristics (i.e., resonant frequency and attenuation at first, third, fifth, and seventh harmonics) of coated MTSM sensors were measured when the sensors were exposed to air (dry) and when covered with a ~4-mm layer of water (wet). The relative changes of resonant frequency of the wet and dry sensors [Δf_{rel} , (1)] are plotted in Fig. 2(a):

$$\Delta f_{rel} = \frac{f_{dry} - f_{wet}}{f_{dry}}, \quad (1)$$

where f_{dry} and f_{wet} indicate resonant frequencies of dry and wet conditions, respectively. Changes in attenuation also were measured but are not reported here.

Two obvious phenomena can be extracted from Fig. 2(a):

- Sample 4A always shows smaller Δf_{rel} than the other samples at all harmonics.
- At higher harmonics (fifth and seventh), Δf_{rel} of Samples 2 and 3 are greater than Sample 1, and Δf_{rel} of Sample 4A is still smaller than Sample 1.

Sample 4A exhibits much less response to water loading at all the tested harmonics. These trends can be explained

based on the hypothesis that, although the macroscopically observed contact angle of water on the SH surfaces are similar, the mechanics of interaction near the water-SH coating interface differ. It is commonly understood that on rough SH surfaces, water does not wet the entire surface at the microscopic or nanoscopic level [4]. Rather at the level of the roughness, water contacts the peaks protruding from the surface but does not penetrate into the valleys, which are filled with air or vapor. For the SH films tested here, the actual penetration depth of the water layer into the valleys of the rough SH surface are dependent on the conditions (surface wettability) of the SH surface, with Sample 4A exhibiting much less interaction (i.e., less water penetration into roughness). At the macroscopic scale, this reduced interaction could be interpreted as effective slip between the liquid and SH surface due to the reduction of the effective contact area [4], [8], [9].

The MTSM responses displayed in Fig. 2(a) show that SH surfaces with similar contact angles can exhibit different mechanical interactions with water. The contact angle of water droplets on the surface of Samples 2, 3, and 4A are similar with approximately 150°, but the response of MTSM sensors to DI water loading of each SH sample are different and are dependent on the harmonics. Different harmonics probe different acoustic penetration depths into the liquid, with higher harmonics more sensitive to liquid trapped in submicron valleys.

Sample 4B was produced from Sample 4A by treatment with UV light for about 30 minutes. This UV/ozone treat-

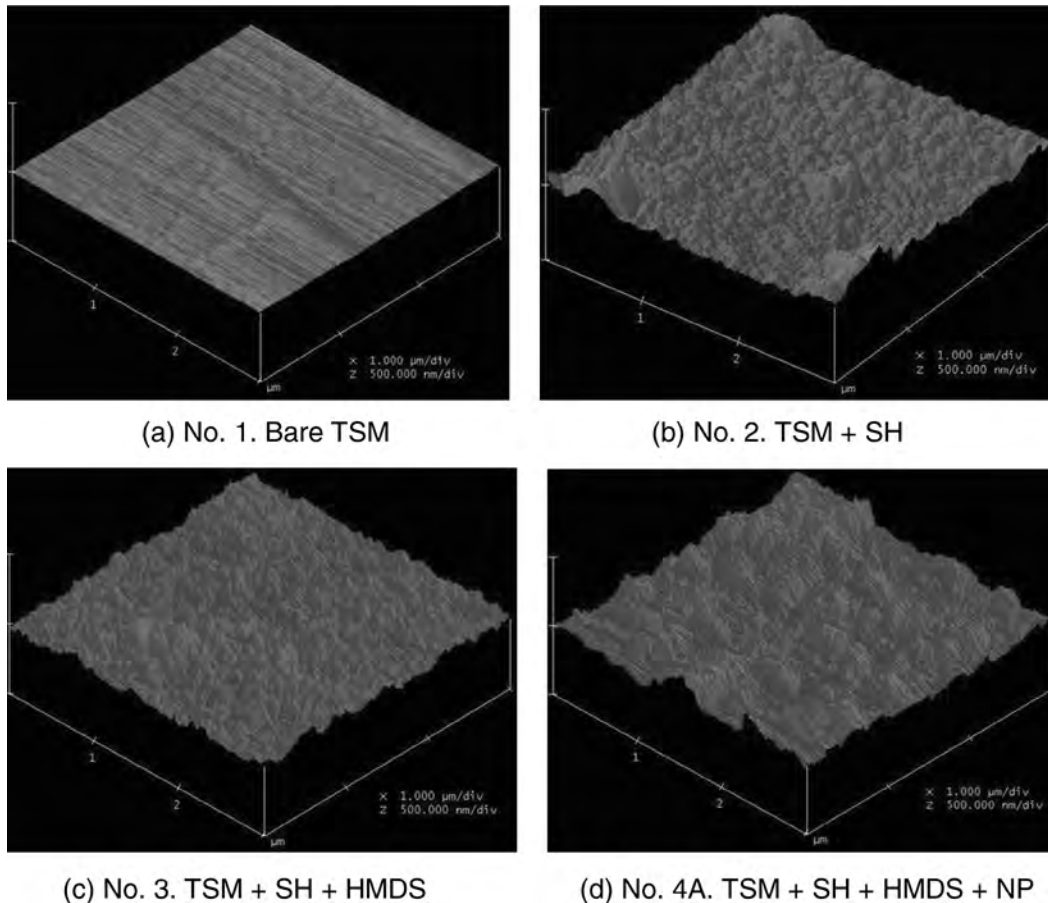


Fig. 1. AFM images of SH films on MTSM sensors. (a) Sample 1, surface of gold electrode on the MTSM sensor; (b) Sample 2; (c) Sample 3; and (d) Sample 4A.

ment does not change the surface morphology; rather it replaces hydrophobic CH_3 and CF_3 groups with hydrophilic hydroxyl groups via an ozone mediated, photo-oxidative process. The contact angle of water on Sample 4B was approximately 90° (see Table I). Again, the frequency responses of Sample 4B were monitored and compared with those of the SH film before UV treatment (Sample 4A) and the bare MTSM (Sample 1). As shown in Fig. 2(b), the relative changes of resonant frequency ($\Delta f_{\text{rel.}}$) of the UV treated sample (Sample 4B) in response to water loading approaches that of the bare MTSM (Sample 1). The $\Delta f_{\text{rel.}}$ curves for Samples 4B and 1 overlap, except for the first harmonic. Although the morphology of the surface of Sample 4B is virtually identical to that of 4A, the surface free energy of Sample 4B is higher than 4A due to the UV treatment as evidenced by the much lower contact angle of water. Higher surface free energy allows water to penetrate deeper into the valleys. Sample 4B senses the additional mass effect from the trapped water and additional viscous damping from the water load on the SH films. Sample 4B shows a similar response to Sample 1 at larger values of resonant frequency.

IV. SUMMARY AND CONCLUSIONS

Three superhydrophobic (SH) and two control surfaces were fabricated by five different processes to produce sur-

faces with varying wettability and submicron scale roughness. The surfaces were characterized with three methods: the acoustic response of MTSM sensors to water loading, nano-scale surface morphology by AFM, and optical measurements of contact angle of water droplets. The AFM measured increases in surface area of 17 to 46% due to roughness of surface treatments. The differences in data were next supported by MTSM results, which also showed the significant differences between those coatings. However, the optical measurements of macroscopic contact angles did not detect differences between the SH coatings. Specifically, the three SH coatings (Samples 2, 3, and 4A), fabricated with and without nanoparticles and with different chemical treatments showed similar macroscopic contact angles; the optical method was capable of only measuring the difference between less hydrophobic Samples 1 and 4B and more hydrophobic Samples 2, 3, and 4A.

Thus, although the contact angles of water droplets are similar on all SH films (samples 2, 3, and 4A), the acoustic method using MTSM sensors clearly exhibited different responses in each sample. It is interesting to notice that the MTSM responses were dependent on the harmonic frequency. Sample 4A showed a much smaller frequency shift under water loading than the other samples; this film incorporated three techniques to provide SH: low free surface energy TFPTMOS coating, HMDS surface treatment,

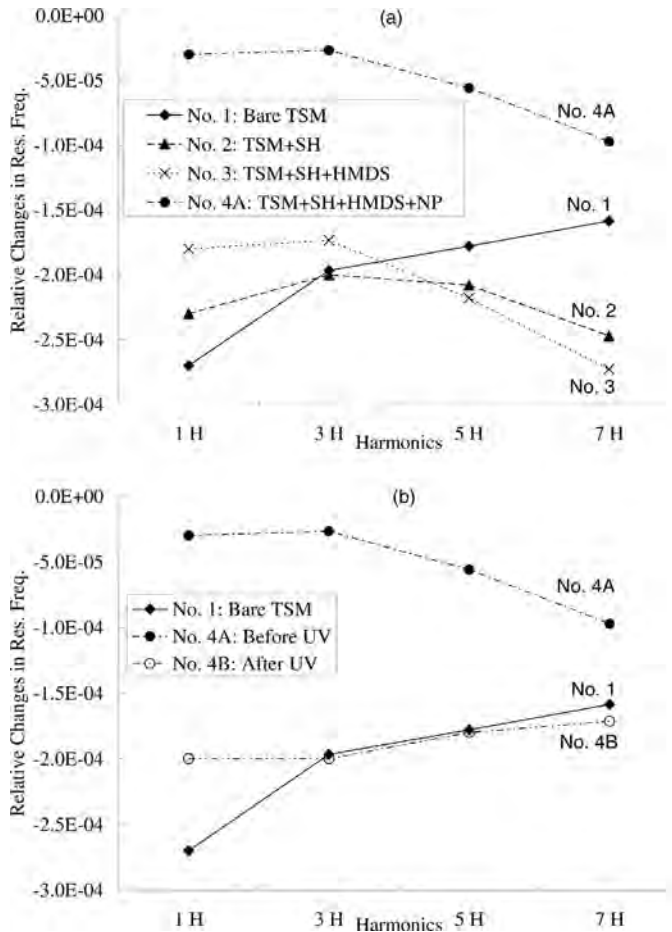


Fig. 2. Relative changes in Δ for (a) MTSM-SH sensors at harmonics, and (b) Sample 4A (before UV), Sample 4B (after UV), and Sample 1 (bare MTSM).

and addition of nano-particles in TFPTMOS. The combination of these factors produces a sample SH coating with the optimized SH properties. These MTSM results can be

interpreted as the presence of effective slip on the textured surface [4].

ACKNOWLEDGMENTS

The authors are pleased to acknowledge the funding support from DOE-Basic Energy Sciences, the Air Force Office of Scientific Research, the Army Research Office, Sandia National Laboratory's LDRD Program, and the National Science Foundation under Grant DBI-0242622.

REFERENCES

- [1] Z. Yoshimitsu, A. Nakajima, T. Watanabe, and K. Hashimoto, "Effects of surface structure on the hydrophobicity and sliding behavior of water droplets," *Langmuir*, vol. 18, pp. 5818–5822, 2002.
- [2] J. Kim and C. Kim, "Nanostructured surfaces for dramatic reduction of flow resistance in droplet-based microfluidics," in *Proc. IEEE Conf. MEMS*, 2002, pp. 479–482.
- [3] L. Zhai, F. C. Cebeci, R. E. Cohen, and M. F. Rubner, "Stable superhydrophobic coatings from polyelectrolyte multilayers," *Nano Lett.*, vol. 4, pp. 1349–1353, 2004.
- [4] S. Gogte, P. Vorobieff, R. Truesdell, A. Mammoli, F. van Swol, P. Shah, and C. J. Brinker, "Effective slip on textured superhydrophobic surfaces," *Phys. Fluids*, vol. 17, pp. 051701-1–051701-4, 2005.
- [5] G. L. Cote, R. M. Lec, and M. V. Pishko, "Emerging biomedical sensing technologies and their applications," *IEEE Sens. J.*, vol. 3, pp. 251–266, 2003.
- [6] K. Rogers, E. Takacs, and M. R. Thompson, "Contact angle measurement of select compatibilizers for polymer-silicate layer nanocomposites," *Polymer Testing*, vol. 24, pp. 423–427, 2005.
- [7] H. Yang, H. An, G. Feng, and Y. Li, "Visualization and quantitative roughness analysis of peach skin by atomic force microscopy under storage," *LWT—Food Sci. Technol.*, vol. 38, pp. 571–577, 2005.
- [8] G. McHale, R. Lucklum, M. I. Newton, and J. A. Cowen, "Influence of viscoelasticity and interfacial slip on acoustic wave sensors," *J. Appl. Phys.*, vol. 88, pp. 7304–7312, 2000.
- [9] G. McHale and M. I. Newton, "Surface roughness and interfacial slip boundary condition for quartz crystal microbalances," *J. Appl. Phys.*, vol. 95, pp. 373–380, 2004.